

Lamb wave ultrasonic evaluation of welded AA2024 specimens at tensile static and fatigue testing

M V Burkov^{1,2,a}, A V Byakov^{1,2}, R T Shah¹, P S Lyubutin^{1,2} and S V Panin^{1,2,b}

¹ Lenina ave 30, National Research Tomsk Polytechnic University, Tomsk, Russia

² Akademicheskii ave 2/4, ISPMS SB RAS, Tomsk, Russia

E-mail: ^aburkovispms@mail.ru, ^bsvp@ispms.tsc.ru

Abstract The paper deals with the investigation of Lamb waves ultrasonic testing technique applied for evaluation of different stress-strain and damaged state of aluminum specimens at static and fatigue loading in order to develop a Structural Health Monitoring (SHM) approach. The experimental results of tensile testing of AA2024T3 specimens with welded joints are presented. Piezoelectric transducers used as actuators and sensors were adhesively bonded to the specimen's surface using two component epoxy. The set of static and cyclic tensile tests with two frequencies of acoustic testing (50 kHz and 335 kHz) were performed. The recorded signals were processed to calculate the maximum envelope in order to evaluate the changes of the stress-strain state of the specimen and its microstructure during static tension. The registered data are analyzed and discussed in terms of signal attenuation due to the formation of fatigue defects during cyclic loading. Understanding the relations between acoustic signal features and fatigue damages will provide us the ability to determine the damage state of the structure and its residual lifetime in order to design a robust SHM system.

1. Introduction

Non-destructive testing (NDT) plays a significant role in development of next generation industry from small watch to huge spacecraft. The most widespread NDT practice of different structures that is used today utilizes defined time intervals of inspection, but the statistics of testing shows that the damages occur in small amount of tested objects while time and funds for diagnostics of the rest were wasted. However the designers cannot expand the inspection intervals because the structures where the damages have been already formed can experience the catastrophic failure which is inappropriate for different industries: aerospace, petrochemical, etc.

To ensure the safe operation of the structure (for example, the passenger aircraft) and simultaneously reduce financial losses during NDT (due to the downtime of the aircraft) scientific and engineering NDT community few years ago focused on research and development of the Structural Health Monitoring (SHM) systems [1,2]. SHM is a non-destructive in-situ sensing and evaluation method that uses a variety of sensors attached to, or embedded in, a structure to monitor the structural response, to analyze the structural characteristics for the purpose of estimating the severity of damage/deterioration and evaluating the consequences thereof on the structure in terms of load bearing capacity and residual lifetime. Various types of data (either continuously or periodically) from the sensors are collected, analyzed and stored for future analysis and reference. The data can be used to identify damage at its onset, to assess strength and integrity, and therefore the performance and safety



of the structure as well as to expand the inspection intervals if the system doesn't register the significant changes exceeding the defined threshold.

There are different SHM principles proposed by different research groups, e.g. strain sensing using optical fiber [3], damage location and identification via the network of ultrasonic transducers embedded in the structure [4] or operational load monitoring using different physical principles and gages [5,6]. All SHM approaches require complex algorithms and software for data processing and decision-making [7] which are based on joint consideration of deformation mechanics of different materials, computer modelling of gages response as well as of the results of experimental verification of SHM technique on different specimens (from small used for mechanical properties evaluation to large structurally similar assemblies). The paper presents the experimental results of Lamb waves ultrasonic evaluation of AA2024T3 specimens with welded joints tested with static and fatigue tension.

2. Materials and methods

The investigation of proposed ultrasonic technique was performed during static and cyclic uniaxial tensile testing of the AA2024T3 specimens with welded joints. The argon arc welding was used for joining process after which the specimens were treated with water quenching at 435°C to reduce residual stress and improve the strength properties of welded joint.

Figure 1 presents the drawing of the dogbone-shaped specimen used for testing. The static tensile testing was performed on electromechanical testing machine Instron 5582 with the load rate of 0.3 mm/min. Cyclic loading with the load ratio $R = 0.1$, 10 Hz loading frequency and P_{max} defined as $0.4\sigma_b$ was performed using servohydraulic testing machine BiSS UTM 150kN. The piezoelectric transducers AW1E12G-190EFL1Z by Audiowell Corp were used as actuators and receivers. These piezoelectric transducers (discs with diameter of 9 mm and thickness of 0.19 mm on steel substrate) were glued on the specimen's surface using 3M Scotch-Weld DP490 epoxy adhesive. The 1st piezoelectric transducer (PZT) was used as an actuator. The 2nd (to characterize the changes outside the highly stressed gage length of the specimen), the 3rd and the 4th (to evaluate the changes in the gage length) were used as receivers. The ultrasonic signals were generated using arbitrary waveform generator AWG-4105 with amplitude of 10 V and frequency in the range from 10 to 500 kHz. The 5-cycle sine modulated by Hanning-window was used as a testing signal.

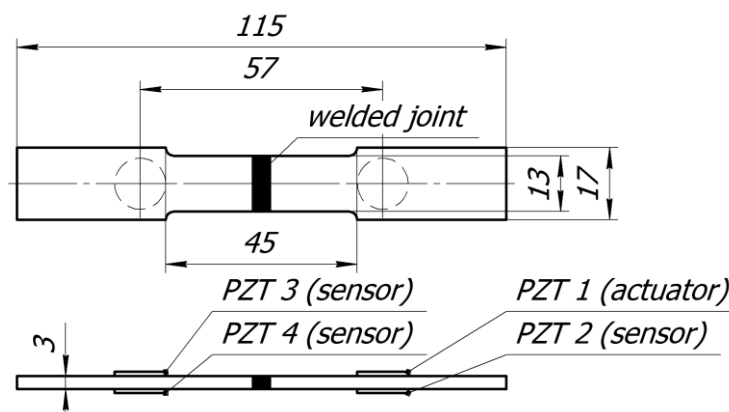


Figure 1. The drawing of the specimen, the position of the PZTs is schematically described.

The signals were recorded using USB oscilloscope Handyscope HS4 with sampling rate of 5 MHz and 12 bit resolution and filtered using band-pass 10-800 kHz filtering. The signal acquisition from sensor PZTs was triggered by the reference signal. The recorded acoustic signals were averaged 100 times and processed to calculate maximum envelope in order to characterize the state of the specimen at different static loads or fatigue lifetime. The calculation of the maximum envelope of received ultrasonic signal was carried out using Hilbert transform procedure in the frequency domain [8].

There are two experiments performed for the uniaxial static tension. In the first the continuous loading was used and the signals were recorded when the loading was stopped – the specimen was fixed in grips and subjected to tensile loads. In the second the loading was performed in the step mode and two signal sets were recorded: in loaded condition and when the load was withdrawn. The main goal of the static tests is to investigate the response of the actuator-receiver pairs during loading and to find the dependence of the sensed signal on the different stress-strain or damaged state. The cyclic loading experiment was carried out in the following manner: after a defined number of cycles the cyclic loading was stopped and the P_{\min} was set to obtain the ultrasonic testing data. Thus the sensed signal amplitude dependence on different lifetime was recorded.

3. Results of static testing and discussion

Our previous work [9] was related to the investigation of the Lamb waves testing applied to unnotched AA2024T3 specimens tested with static and fatigue tension. Herein the same testing technique was applied and the same two testing frequencies (50 and 335 kHz) were used. The results of the present paper are quite similar to those obtained earlier.

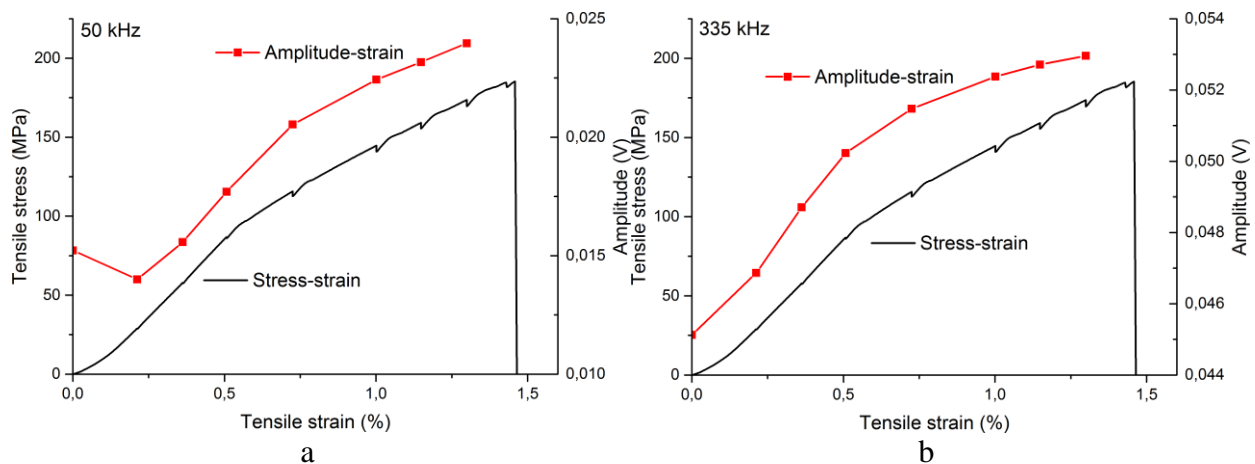


Figure 2. Combined stress-strain and amplitude-strain graphs for the continuous tension test of the welded AA2024T3 specimen.

Figure 2 represents two combined graphs of the stress-strain curve of the AA2024T3 specimen with welded joint loaded continuously until fracture and the amplitude of the signal sensed by the 3rd PZT located on the same side with the generator along the gage section of the specimen. The signal sensed by the 4th PZT is almost the same with the 3rd except the reverse sign of the instantaneous sensed signal magnitude due to the propagation of A_0 Lamb wave mode. There are 7 points of defined load values where the loading was stopped and the ultrasound testing was performed (these points are easily recognized as the teeth on the stress-strain curve due to the stress relaxation during data acquisition). The first graph (a) corresponds to the frequency of 50 kHz; the second (b) to the 335 kHz. It is seen that amplitude of both high and low frequency signals increases during loading of the specimen. This result is similar to one obtained in the previous our work that the ultrasound used is sensitive to the different stress-strain state. After the second experiment two sets of data were obtained because loading was performed in step mode with data acquisition at both loaded and unloaded conditions. The different testing procedure with the stress relaxation occurring during unloading of the specimen results in different propagation of ultrasound during whole experiment. Figure 3 presents two curves: while the specimen was in loaded (red square) and unloaded (black triangle) conditions. Graph (a) corresponds to the low frequency signal and (b) to the high frequency.

It is seen that in contrast to the first experiment the amplitude (loaded state – red square plot) for both high and low frequency testing decreases during extension of the specimen. The amplitude for the low frequency signal starts to decrease from the initial of loading with constant slope till the 1.1 % of

tensile strain. Then short nonlinear stage is observed and finally there are three last points with constant amplitude value captured till the specimen fracture. The amplitude of the high frequency signal propagated along the gage length stays constant till 0.8 % of strain and then it starts to decrease nonlinearly up to fracture. The correspondent curves of amplitude recorded in the unloaded condition are plotted on the same graph (black triangle) and they have the same shape compare to the plots recorded in the loaded state. However there are small differences:

- the amplitude of high frequency signal start to decrease after the strain reaches higher values (~1.3 %);
- low frequency signal has lower amplitude throughout all the experiment and its amplitude increases slightly near fracture.

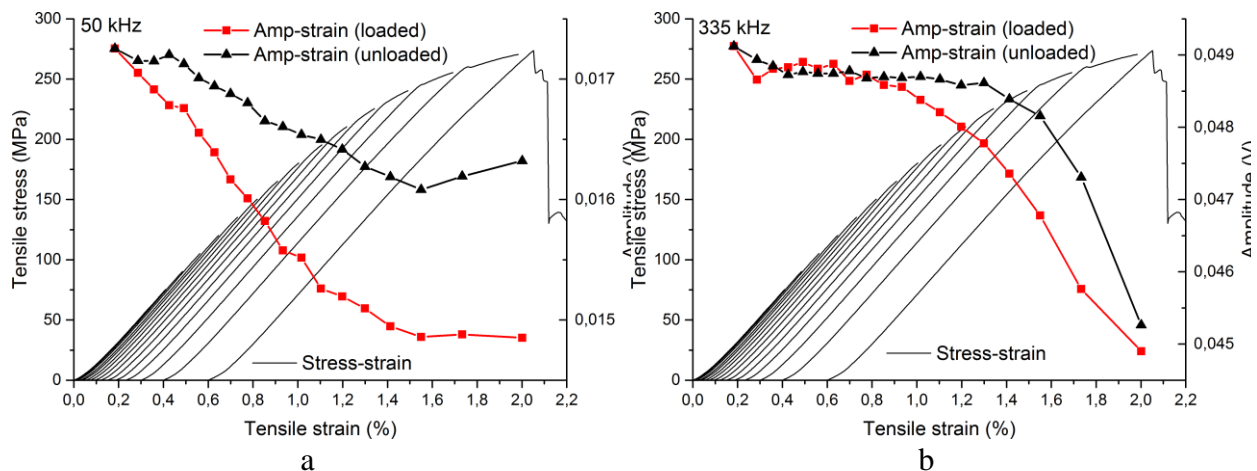


Figure 3. Combined stress-strain and amplitude-strain graphs for the step-mode tension test of the welded AA2024T3 specimen.

By analyzing the data obtained in our previous work [9] it can be noted that both high and low frequency signal propagation behavior during step mode loading of welded AA2024T3 specimen obtained in the present paper were the same compared to the unnotched specimen tested before. Low frequency signal amplitude decreases from the initial of loading and stays constant up to fracture while high frequency sensed signal decreases rapidly after the 2/3 of tensile strain.

4. Results of cyclic testing and discussion

Based on the results obtained during static tensile experiments the parameters for cyclic investigation were chosen. The average ultimate tensile stress for three specimens was obtained (210 MPa) and the maximum stress for cyclic was estimated as $0.4\sigma_u=82$ MPa. Thus three data sets for specimens with lifetime of 9000 cycles, 33500 cycles and 84000 cycles were captured. Such huge scatter of the lifetime is the result of poor quality of welded joints but it was not a problem for the present research where the ultrasonic testing technique was investigated. Moreover the presence of large welding defects such as pores or inclusions can give rise to the formation of large crack during cyclic loading in order to assess the Lamb wave testing technique sensitivity. The testing and data acquisition technique in this section are similar to ones used in static testing: there are two frequencies of testing 50 and 335 kHz, the amplitude of sensed signal corresponds to the 3rd transducer located on the same side with generator along the gage section of the specimen.

Figure 4 presents two graphs of low (a) and high (b) frequency signal amplitude registered during cyclic loading of the specimen fractured after only 9000 cycles. Because the data acquisition interval was set to 2000 cycles there are only four points were captured. Low frequency signal amplitude behaves uncertainly while the high frequency amplitude remains constant at first three points and then large decrease is registered. Low amount of data capturing points doesn't allow us to make any precise

analysis of the propagated signal behavior so let's consider the second specimen with 33500 cycles of lifetime (Figure 5).

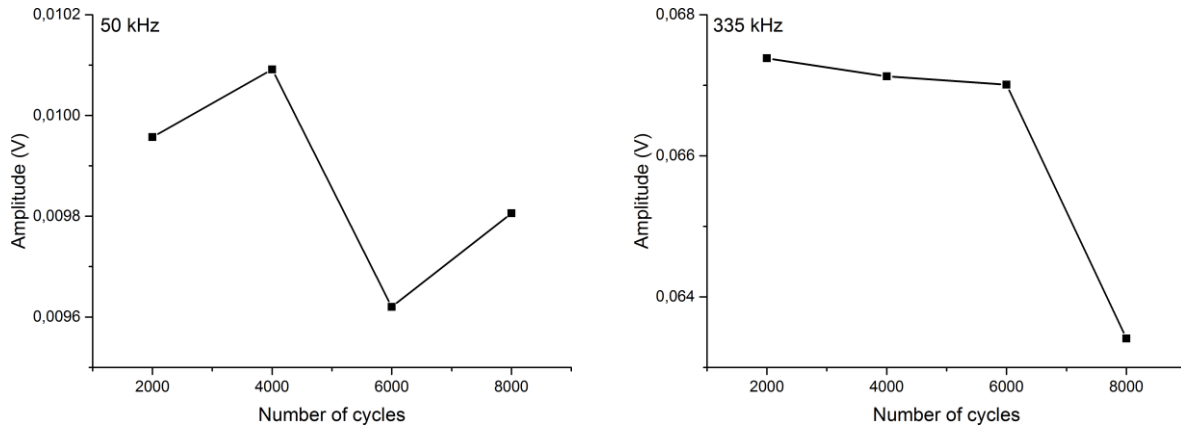


Figure 4. Sensed signal amplitude dependence on the different number of cycles for the specimen with lifetime of 9000 cycles.

It is seen that low frequency sensed signal graph doesn't have any precise trend during cyclic loading. The plot has large hops and drops of amplitude magnitude while the average value stays constant. In contrast to the low frequency behavior the high frequency signal amplitude decreases monotonically from the initial of the experiment till fatigue failure of the specimen.

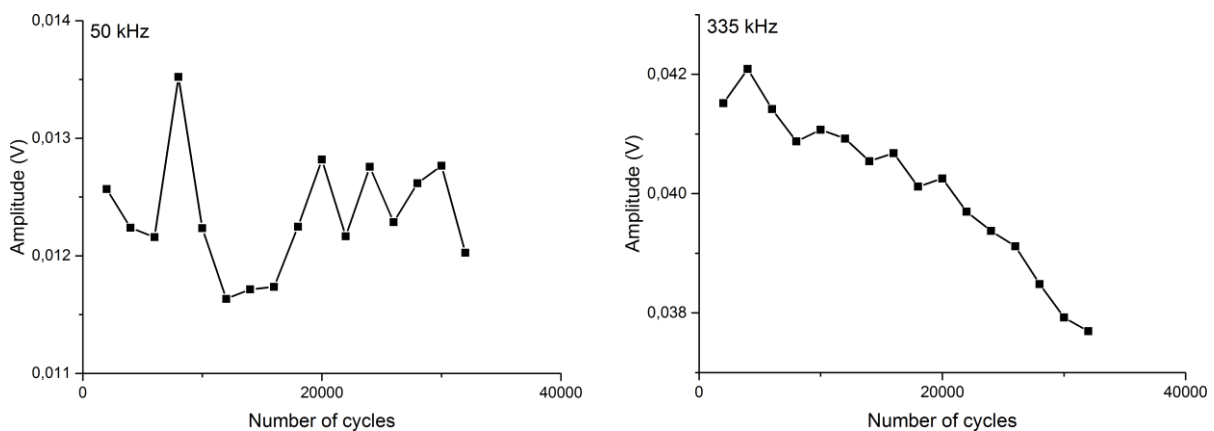


Figure 5. Sensed signal amplitude dependence on the different number of cycles for the specimen with lifetime of 33500 cycles.

Figure 6 presents the graphs of amplitude for the specimen with lifetime of 84000 cycles. The amplitude value for the low frequency testing stays near constant during entire experiment and at the last point near fracture the large jump is registered. This result differs with the explanation according to which the amplitude should decrease due to the higher signal attenuation owing to the micro damaging of the structure or the large crack formation. The second graph for high frequency confirms the assumption of higher attenuation with large drop of the sensed signal amplitude registered at the last point before fatigue failure. Also it should be noted that the specimen withstand more than 1500 cycles of load after the last data acquisition point.

5. Conclusion

The analysis of the obtained results allows us to conclude that the ultrasonic testing technique is sensitive to the different stress-strain state which appears in the increase of sensed signal amplitude

during continuous tension test. This increment for both frequencies can be explained like a string being subjected to tension conducts elastic waves with lower attenuation. During the step mode tensile test where due to the stress relaxation after unloading the internal structure of the specimen exhibits significant changes. So based on the results of the present test the following can be concluded: the amplitude of both high and low frequencies decreases during extension of the specimen that is related most likely to the formation of the macro-defects in the welded joint that result in higher attenuation of the sensed signal.

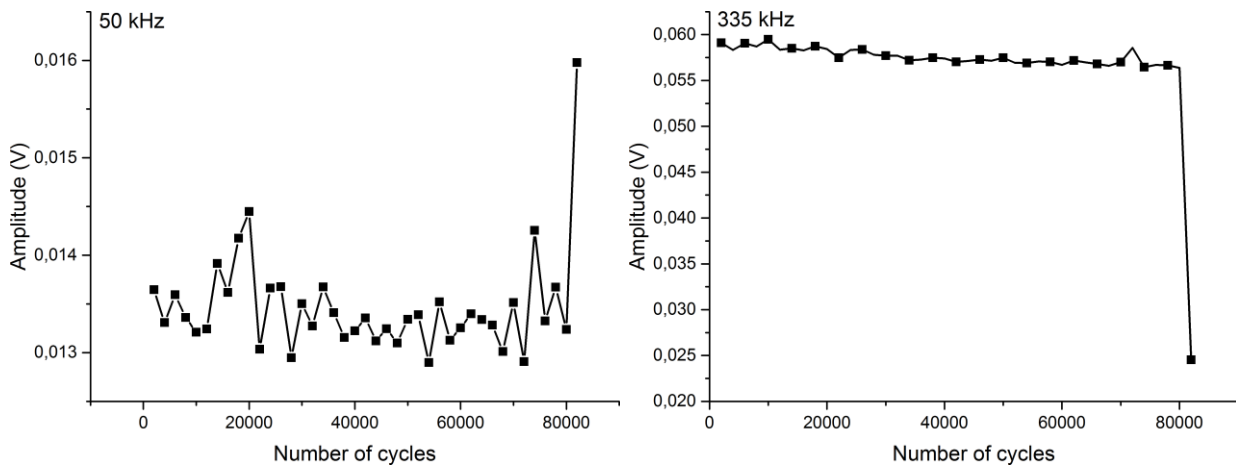


Figure 6. Sensed signal amplitude dependence on the different number of cycles for the specimen with lifetime of 84000 cycles.

The analysis of the fatigue tension test allows us to conclude that during cyclic loading the structure of the tested specimen exhibits the changes which influence the signal propagation. While the behavior of the graphs of low frequency signals amplitude is uncertain and cannot be interpreted in a precise manner the high frequency amplitude graphs behavior for the specimens with different lifetimes is similar to each other: the amplitude value decreases during whole cyclic loading. Thus we can conclude that only high frequency testing provides the results that can be interpreted accurately in order to design a SHM technique. The next our investigation will be related to the application of the present ultrasonic technique for evaluation of aluminum specimen during high-cycle fatigue (up to 1M cycles).

Acknowledgements

The work is supported by the RFBR grants № 13-07-00009_a and № 14-08-31747 mol_a.

References

- [1] P J Schubel, R J Crossley, E K G Boateng and J R Hutchinson 2013 *Renew. Energ.* **51** 113-123
- [2] W Liu, B Tang and Y Jiang 2010 *Renew. Energ.* **35** 1414-1418
- [3] S Minakuchi, Y Okabe, T Mizutani and N Takeda 2009 *Smart Mater. Struct.* **18** 9
- [4] Q Lei, Y Shenfang, W Qiang, S Yajie and Y Weiwei 2009 *Chinese J. Aeronautics* **22** 505-512
- [5] P Wang, T Takagi, T Takeno and H Miki 2013 *Sensors and Actuators* **198** 46- 60
- [6] S V Panin, M V Burkov, P S Lyubutin, Yu A Altukhov and I V Shakirov 2014 *Engineering Fracture Mechanics* **129** 45-53.
- [7] Ch E Katsikeros and G N Labeas 2009 *Mechanical Systems and Signal Processing* **23** 372-383
- [8] S L Hahn 1996 *Hilbert Transforms in Signal Processing* (Norwood: Artech House)
- [9] A V Byakov, A V Eremin, M V Burkov, R T Shah, P S Lyubutin and S V Panin *Applied Mechanics and Materials* – in press.